SPH ANALYSIS OF INKJET DROPLET IMPACT DYNAMICS

T. TILFORD*, J. BRAUN†, J. C. JANHSEN†, M. BURGARD†, C. BAILEY*

*Computational Mechanics and Reliability Group, University of Greenwich, UK
Email T.Tilford@gre.ac.uk

† Fraunhofer-Institut für Produktionstechnik und Automatisierung, Germany

Key words: SPH, Additive Manufacturing, Microelectronics, Microfluidic Analysis

Abstract. This paper presents a novel Smoothed Particle Hydrodynamics (SPH) framework for analysis of droplet impact dynamics in a 3D inkjet printing process. Results obtained are validated against experimentally derived high-speed imaging data. The numerical framework is based on the Smoothed Particle Hydrodynamics approach of Monaghan et al [1] which has been proven to be efficient and effective for analysis of dynamic fluid flow problems involving free surface interfaces. The SPH approach has been augmented through addition of the kernel gradient correction scheme proposed by Belytschko et al [2] and stabilization terms of Marrone et el [3]. This correction provides a more accurate approximation of the boundary forces including surface tension which dominate at typical inkjet droplet lengthscales (<100 µm). Analysis is expedited through adoption of the OpenACC programming paradigm to enable GPU based computation.

Numerical analyses have been validated against analytical solutions, reference macroscale problems and through comparison with experimental high speed imaging data of the inkjet printing process. The experimental setup consisted of a Fuji Dimatix SL-128 inkjet printhead jetting an acrylate based 3D printing build material onto a glass substrate. Images of a single inkjet droplet impacting onto the glass slide were captured at a rate of 100,000 frames per second, with droplet diameter assessed using a weight test approach.

Qualitative comparison of the numerical and experimental results showed a good agreement, indicating that the implemented framework is effective for analysis of the fluidic aspects of the printing process. The model is able to assist in tackling manufacturing issues that can detrimentally influence the quality of manufactured parts through provision of insight into the process.

1 INTRODUCTION

Additive manufacturing is becoming widely adopted across a range of industrial sectors and being applied to increasingly high value and high complexity products. Piezoelectric drop-on-demand inkjet printing systems can be used to form truly three dimensional, multi material objects with very high dimensional accuracy. The development of conductive pastes that can be dispensed using inkjet printers has enabled the approach to be utilised for development of microelectronics components.

The large number of academic research 3D printing systems targeting the electronics packaging sector [4-6] are now augmented by a number of commercially available systems intended for production of saleable products such as the Nano Dimension Dragonfly [7] and the Optomec [8] systems. The EU funded NextFactory [9-11] project has developed a 3D printing, micro-deposition, micro-assembly, and curing system, illustrated in Figure 1a, that can accurately deposit and cure both functional and structural materials and place/embed components in an integrated manner within a single platform. The system uses a hybrid approach in order to increase its flexibility, with an inkjet system augmented by microdeposition tools that enable conductive adhesive materials to be used alongside silver nano-inks for conductive features.

The system enables producers of micro-mechatronic systems to manufacture complete products on a single machine with the manufacturing process from CAD design to finished product taking a number of hours rather than more lengthy timescales typically associated with traditional manufacturing methods. The three-dimensional nature of the build process enables manufacture of complex 3D microsystems as readily as 2D and 2.5D devices.

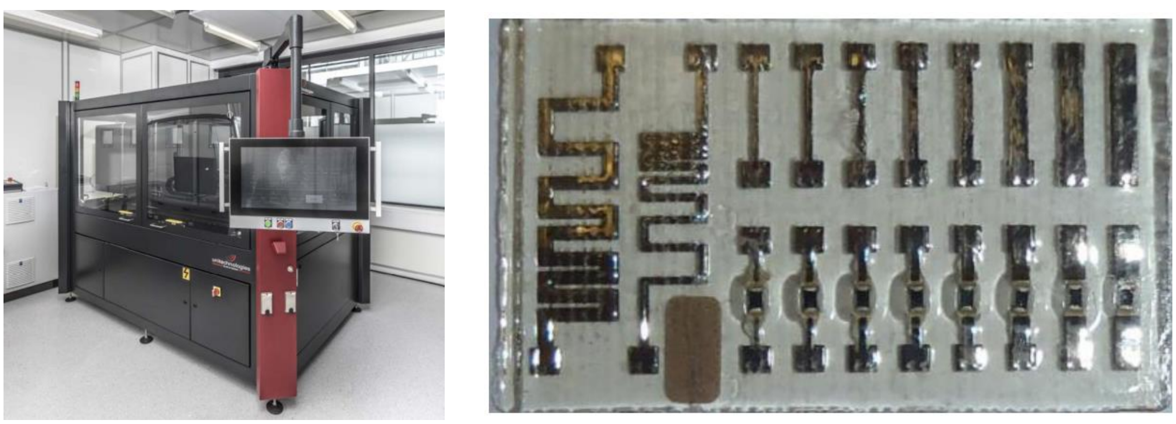

Figure 1(a): NextFactory 3-D additive manufacturing system and 1(b) 3-D printed microelectronics test structure

As is the norm for the electronics sector, new manufacturing approaches need to be considered in terms of the long term reliability of the final product. In addition to commonplace reliability qualification approaches such as JEDEC tests, there is an increasing drive to assess component quality during the manufacturing process. Condition based monitoring approaches measure key parameters associated with component quality during manufacture and continually optimise process parameters in real time to increase final quality and reliability of formed components [12, 13]. Such condition based monitoring systems need to be trained as to how variation of process parameters influences product quality. A numerical model, capable of detailed analysis of the process, can be used to underpin such an approach.

The primary requirement of the numerical model for inkjet deposition is to capture the complex physics involved when and inkjet droplet impacts a printed surface. There are a number of significant challenges in such an analysis. The primary challenge is that analysis of droplet impact upon an idealised flat surface is insufficient. Only the first layer of an inkjet printed structure will be deposited on the flat baseplate. The following layers will be deposited onto a layer of partially cured polymer droplets which form and uneven surface and will deform on impact. The material is not a simple Newtonian fluid such as water but a complex multi-component polymer which exhibits shear dependent viscous behaviour – a complex non-Newtonian material. Additionally, the impact is very severe with a droplet of diameter in the order of 40 microns impacting at approx. 5 metres per second.

Traditional computational fluid dynamics (CFD) approaches such as the Finite Volume Method [14] would be readily capable of modelling the impact dynamics of a small number of droplets. However, in order to consider prediction of the development of defects over a number of layers it is necessary to take advantage of a more efficient approach such as GPU enabled SPH. This approach has a number is advantages over traditional methods in that interfaces are explicitly captured rather than needing to be approximated but, more critically, incorporates a finite support distance enabling the problem domain to be subdivided into a large number of overlapping subdomains which can be assessed on a single core of a graphical processor unit.

2 Numerical Approach

The Smoothed Particle Hydrodynamics (SPH) approach was developed by Lucy [15] and by Gingold and Monaghan in 1977 [1]. It is a versatile discrete particle method for solution of a number of differing physical phenomena. It is a computationally highly effective method for solution of complex fluid flows, particularly in cases with interfaces and large deformations. The SPH approach considers the fluid as a collection of particles, each associated to a number of physical properties such as position, velocity, mass, density, etc. At the heart of the SPH approach is a means of evaluating spatial derivatives through integral interpolants which use kernels to approximate a delta function. The integral interpolant of any quantity function A(r) is defined by:

$$A(r) = \int_{\Omega} A(r')W(r - r', h)dx \quad (1)$$

This relates the value of parameter A, a scalar variable such as pressure, at location r, through integration of the value of A over surrounding space Ω with a smoothing kernel W. This smoothing kernel essentially acts as a weighting factor which, critically, enables the variation of A at distances greater than a defined value to be ignored. This finite support radius enables the physical domain to be subdivided into a number of overlapping subdomains which greatly enhances the computational efficiency of the approach. In the standard SPH formulation, this can be written as:

$$A_i(r) = \sum_j A_j \frac{m}{\rho} W(ri - rj, h) \tag{2}$$

In which the value of A of particle i is evaluated by summing the values of A at all particles within the support radius as a function of their mass, m, density, ρ and kernel, W. This can be extended to spatial derivatives through the following functions:

$$\nabla A_i(r) = \sum_j A_j \frac{m}{\rho} \nabla W(ri - rj, h) \tag{3}$$

$$\nabla^2 A_i(r) = \sum_j A_j \frac{m}{\rho} \nabla^2 W(ri - rj, h) \tag{4}$$

A number of different kernels have been proposed in SPH literature, each with differing behaviour benefits and drawbacks. The cubic spline kernel has been adopted for this analysis as it is the most widely used and understood. The Cubic spline is given by the following function, with normalisation factors, σ, of 1/h, 10/(7πh2), and 1/(πh3) in one, two and three dimensions respectively.

$$W(r,h) = \sigma \begin{cases} 1 - \frac{3}{2}q^2 + \frac{3}{4}q^3 & 0 \le q \le 1 \\ \frac{1}{2}(2-q)^3 & 1 \le q \le 2 \\ 0 & q > 2 \end{cases} \tag{5}$$

This limited support radius enables the solution domain to be subdivided into cell each with dimension equal to the support radius. When each cell is linked with the 26 surrounding cells to form a sub-region, the domain is separated into a number of overlapping subdomains in that a particle inside the subregion will only have a valid interaction with particles in the same region as particles in other regions will be more than the support radius away. This is a key advantage of the SPH approach in that the computational cost of solving a number of small problems is significantly lower than solving one very large problem. Additionally, the numerical processing can be performed on a graphical processing unit (GPU) which comprises a relatively large number of relatively small cores which is ideally suited to such problems.

Within each subdomain it is necessary to determine the movement of each particle as a function of the acceleration due to interaction forces from surrounding particles. The fluid flow forces are governed by the Navier Strokes Equations, which can be written as:

$$\frac{\delta}{\delta t}(\rho u) + (\rho u \cdot \nabla) = -\nabla p + \mu \nabla^2 u + g \tag{6}$$

In the SPH approach these can be reformulated as a smoothed interaction force between each pair of particles. The acceleration of a particle can therefore be derived through summation of these forces over all particles within the support radius. The total acceleration force can be written as:

$$\frac{\delta \rho_i}{\delta t} = -\rho_i \sum_j (u_j - u_i) \cdot \nabla W(r_i - r_j, h) \frac{m_i}{\rho_i} \tag{7}$$

$$\frac{\delta}{\delta t}(\rho u_i) = -\sum_j m_j \left[\left(\frac{p_i}{\rho_i^2} + \frac{p_j}{\rho_j^2} \right) - \frac{\varepsilon}{\rho_i \rho_j} \frac{4\mu_i \mu_j}{(\mu_i + \mu_j)} \frac{u_{ij} \cdot r_{ij}}{r_{ij}^2 + \eta^2} \right] \nabla W(r_i - r_j, h) \tag{8}$$

In addition to the standard SPH formulation, a number of additional functions needed to be implemented in order to address specific challenges of the inkjet droplet impact problem. The first of these is to implement the dissipative SPH framework of Marrone et al [3] in order to better deal with the violent impact events. This framework involves modification of the interaction forces to incorporate additional stabilisation terms such that:

$$\frac{\delta \rho_i}{\delta t} = -\rho_i \sum_i (u_j - u_i) \cdot \nabla W(r_i - r_j, h) \frac{m_j}{\rho_j} + \delta h c_0 \sum_j \psi_{ij} \cdot \nabla W(r_i - r_j, h) \frac{m_j}{\rho_j} \tag{9}$$

where:

$$\psi_{ij} = 2(\rho_j - \rho_i)\frac{r_{ji}}{|r_{ij}|^2} - [(\nabla\rho_i) + (\nabla\rho_j)] \tag{10}$$

$$\pi_{ij} = \frac{(-u_i)\cdot r_{ji}}{|r_{ij}|^2} \tag{11}$$

The XSPH correction of Monaghan [16] has been implemented to stabilise the analysis, which modifies the particle velocity based on the velocity of the surrounding particles in a manner given by:

$$\frac{\delta r_i}{\delta t} = u_i + \varepsilon \sum_j \frac{m_{bj}}{\bar{\rho}_{ij}} u_{ji}\, W(r_i - r_j, h) \tag{12}$$

Furthermore, the kernel gradient correction approach of Belytschko [2] is implemented to correct the evaluation of the kernel and gradient values at interfaces. In these regions the support radius covers a region of liquid, represented by particles, and a region of air which, in this implementation, is represented by an absence of particles. The approach of Belytschko requires a 4x4 matrix to be inverted in order to determine the correction factors however this increases the accuracy of the analysis in the critical impact phase of the process. Time integration has been handled through use of a velocity Verlet scheme [17] while material cure behaviour has been handled through a viscosity modification term. A more detailed analysis of the cure kinetics and the non-Newtonian rheometry of the jetted fluids are required to improve the accuracy of the model.

$$\boldsymbol{A} = \sum_j W_i^s \begin{bmatrix} 1 & \delta x & \delta y & \delta z \\ \delta x & \delta x\delta x & \delta y\delta x & \delta z\delta x \\ \delta y & \delta x\delta y & \delta y\delta y & \delta z\delta y \\ \delta z & \delta x\delta z & \delta y\delta z & \delta z\delta z \end{bmatrix} \tag{13}$$

$$\mathrm{A}\alpha = \mathrm{I} \tag{14}$$

$$\mathrm{W}_i^s = \frac{W_i}{\sum_j \left(\frac{m_j}{\rho_j} W_j\right)} \tag{15}$$

$$W = \alpha_{11} + \alpha_{12}\delta x + \alpha_{13}\delta y + \alpha_{14}\delta z \tag{16}$$

$$\nabla W_x = \alpha_{21} + \alpha_{22}\delta x + \alpha_{23}\delta y + \alpha_{24}\delta z \tag{17}$$

$$\nabla W_y = \alpha_{31} + \alpha_{32}\delta x + \alpha_{33}\delta y + \alpha_{34}\delta z \tag{18}$$

$$\nabla W_z = \alpha_{41} + \alpha_{42}\delta x + \alpha_{43}\delta y + \alpha_{44}\delta z \tag{19}$$

3 Droplet Impact Analysis

Analysis of a single droplet of uncured polymer has been performed using the model. The analysis has considered an initial state of a perfectly spherical droplet of diameter 23µM travelling toward a flat plane at 5 Ms-1. The fluid is considered to have constant viscosity of 0.015 Pa.S and density 1000.0 KgM-3. Surface energy values for the fluid-air interface and fluid surface interface were taken as 72 mJM-2. Polymer materials typically exhibit non-Newtonian behavior and the surface energy behavior is more complex than considered in the model and as such the accuracy of the analysis will be limited until the model is extended to capture these phenomena.

The development of the droplet shape during the impact, as predicted by the numerical model, is illustrated in Figure 2. The six images show the droplet at 1, 10, 20, 86, 200 and 400 µs after impact. The high impact speed causes relatively localized deformation in the immediate post impact phase before the kinetic energy is transferred into transverse momentum and significant viscous energy dissipation. The point at which the droplet has greatest transverse radius occurs at 86 µs, where momentum forces have been balanced by the surface tension forces resulting in zero velocity at the outermost extents of the droplet. Beyond this time, the surface tension forces draw the droplet back into a more spherical shape as shown in in the 200 and 400 µs plots.

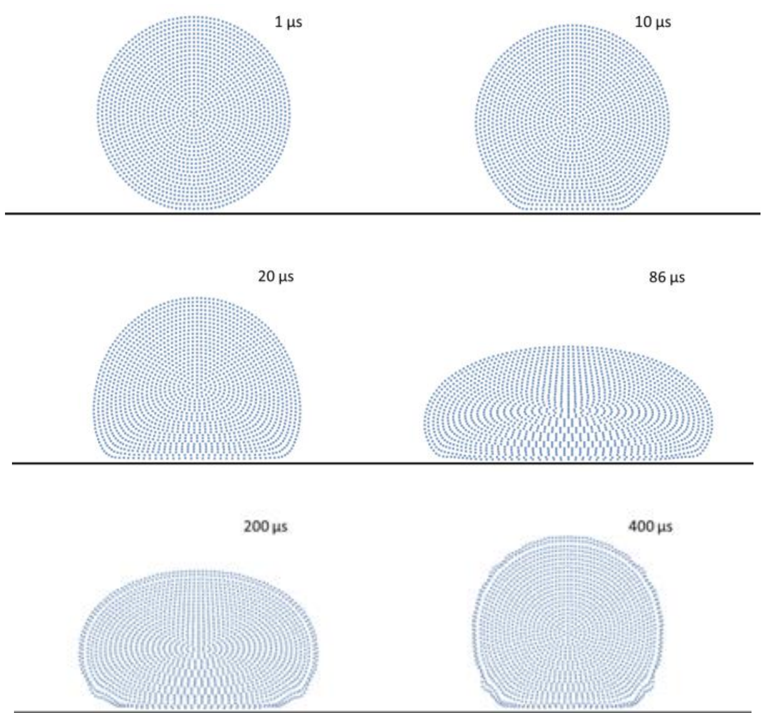

Figure 2: Single droplet impact sequence

These numerical results can validated through qualitative comparison with high speed imaging data. The experimental setup consisted of a Fuji Dimatix SL-128 inkjet printhead jetting an acrylate based 3D printing build material onto a glass substrate. Images of a single inkjet droplet impacting onto the glass slide were captured at a rate of 100,000 frames per second, with droplet diameter being accurately assessed using a weight test approach. Figure 3 illustrates a droplet impact sequence showing on in every three images for conciseness. Comparison of these he images with numerically derived results would suggest a discrepancy between the actual surface tension values and those considered in the model.

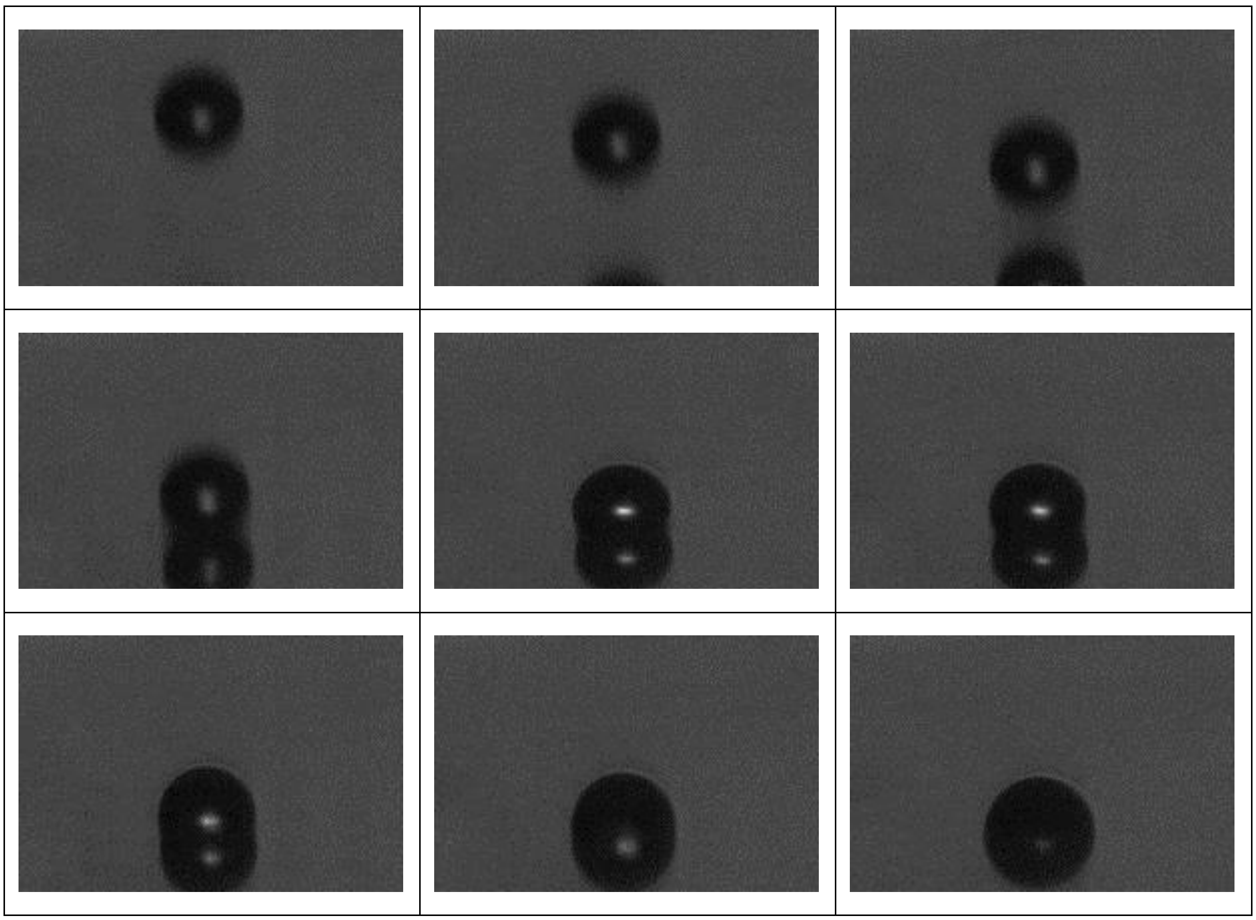

Figure 3: High-speed imaging droplet impact sequence

5 Conclusions

A new, effective approach for analysis of droplet impact dynamics associated with piezoelectric drop-on-demand inkjet printing systems was presented. The SPH formulation of Lucy and Gingold and Monaghan has been used as the basis for the model, with the δ-SPH terms of Marrone et al and gradient correction terms of Belytschko used to improve the accuracy and stability.

Qualitative comparison of results obtained from the numerical framework with experimentally derived high speed imaging data show the applicability of the approach. The approach could be further enhanced by implementation of an iterative incompressible approach such as that proposed by Ihmsen et al [18] and through integration of an appropriate cure kinetics model to capture post impact UV cure processes.

Acknowledgements

This paper is based on work supported by the NextFactory research project funded under the European Community´s 7th Framework Programme (FP7/2007-2013) under grant agreement No. 608985 and through University of Greenwich REF/PP funding

REFERENCES

[1] Monaghan, J. J., “On the Problem of Penetration in Particle Methods”. Journal Computational Physics, Vol. 82, pp. 1-15, 1989

[2] Belytschko, T., Krongauz, Y., Organ, D., Fleming, M., “Meshless methods: an overview and recent developments”, Computer Methods in Applied Mechanics and Engineering, Vol. 139, Issues 1–4, pp. 3-47, 1996

[3] Marrone, S., Antuono, M., Colagrossi, A., Le Touzé, D., Graziani, G., “δ-SPH Model for Simulating Violent Impact Flows”, Computer Methods in Applied Mechanics and Engineering. Vol. 200, pp. 1526–1542, 2011

[4] Kawahara,Y., Hodges, S., Cook, B. S., Zhang, C., Abowd, G. D., “Instant inkjet circuits: lab-based inkjet printing to support rapid prototyping of UbiComp devices”, Proc UbiComp’13, September 8–12, 2013, Zurich, Switzerland, pp. 363-372

[5] B. Khorramdel, J. Liljeholm, M. Laurila, T. Lammi, G. Mårtensson, T Ebefors, F. Niklaus, M.Mäntysalo, Inkjet printing technology for increasing the I/O density of 3D TSV interposers, Microsystems and Nanoengineering, Vol. 3, 10.04.2017, p. 17002.

[6] Integration of inkjet and RF SoC technologies to fabricate wireless physiological monitoring system, H Sillanpää, A Vehkaoja, D Vorobiev S Nurmentaus, J Lekkala, M Mäntysalo, Proc. 5th Electronics System-integration Technology Conference (ESTC), Helsinki, 2014, doi:10.1109/ESTC.2014.6962739

[7] http://www.nano-di.com [Accessed: 31 May 2018].

[8] M O'Reilly and Jeff Leal, Jetting your way to fine pitch 3D interconnects, Chip Scale Review, Sept/Oct 2010

[9] NextFactory, http://www.nextfactory-project.eu [Accessed: 31 May 2018].

[10] Guenthel, J., Holzinger, D., Birch, R., Refle, O., "Process & Machine Development for the Integration of Conductive Paths Inside a 3D Printed Microsystem", Proc. Direct Digital Manufacturing Conference, Berlin, Germany, 2016

[11] Tilford, Timothy, Stoyanov, Stoyan, Braun, Jessica, Janhsen, Jan Cristophe, Burgard, Matthias, Birch, Richard and Bailey, Christopher (2018) Design, manufacture and test for reliable 3D printed electronics packaging. Microelectronics Reliability, 85. pp. 109-117. ISSN 0026-2714 (doi:10.1016/j.microrel.2018.04.008)

[12] Tourloukis, G., Stoyanov, S., Tilford, T., Bailey, C., "Data driven approach to quality assessment of 3D printed electronic products", Proc. 38th International Spring Seminar on Electronics Technology, 2015, pp. 300 – 305

[13] S. Stoyanov, C. Bailey, Machine learning for additive manufacturing of electronics, 40th International Spring Seminar on Electronics Technology (ISSE), 2017

[14] Patankar, Suhas V., Numerical Heat Transfer and Fluid Flow, McGraw-Hill, 1980

[15] Lucy, L., "A numerical approach to testing the fission hypothesis", Journal Astronomical., Vol. 82, pp. 1013-1924, 1977

[16] Gingold, R. A., Monaghan, J. J., "Smoothed Particle Hydrodynamics: Theory and Application to non-Spherical Stars" Mon. Not. R. Astr. Soc., Vol. 181, pp. 375-389, 1977

[17] L. Verlet, "Computer Experiments on Classical Fluids, I: Thermodynamical Properties of Lennard-Jones Molecules. Phys Rev, Vol. 159, pp. 98–103, 1967

[18] M. Ihmsen, J. Cornelis, B. Solenthaler, C. Horvath, M. Teschner, Implicit Incompressible SPH, IEEE Transactions on Visualization and Computer Graphics, July 2013.